Single-phase Whole-body 64-MDCT Split-bolus Protocol for Pediatric Oncology: Diagnostic Efficacy and Dose Radiation

MICHELE SCIALPI[1], RAFFAELE SCHIAVONE[2], ALFREDO D'ANDREA[3], ISABELLA PALUMBO[4], MICHELLE MAGLI[5], SABRINA GRAVANTE[1], GIUSEPPE FALCONE[1], CLAUDIO DE FILIPPI[2] and BARBARA PALUMBO[6]

Department of Surgical and Biomedical Sciences, Division of [1]Radiology 2, [3]Radiotherapy and [6]Nuclear Medicine, Santa Maria della Misericordia Hospital, Perugia University, Perugia, Italy;
[2]Division of Radiology, Meyer Pediatric Hospital, Florence, Italy;
[4]Division of Radiology, San Giuseppe Moscati Hospital, Aversa, Caserta, Italy;
[5]Department of Diagnostic Medicine, Division of Radiology, Santa Maria Hospital, Borgo Val di Taro, Parma, Italy;
[7]Department of Radiological Sciences, Oncology and Pharmacology, La Sapienza University, Rome, Italy

Abstract. *Purpose: To evaluate the image quality and the diagnostic efficacy by single-phase whole-body 64-slice multidetector CT (MDCT) for pediatric oncology. Patients and Methods: Chest-abdomen-pelvis CT examinations with single-phase split-bolus technique were evaluated for T: detection and delineation of primary tumor (assessment of the extent of the lesion to neighboring tissues), N: regional lymph nodes and M: distant metastasis. Quality scores (5-point scale) were assessed by two radiologists on parenchymal and vascular enhancement. Results: Accurate TNM staging in term of detection and delineation of primary tumor, regional lymph nodes and distant metastasis was obtained in all cases. On the image quality and severity artifact, the Kappa value for the interobserver agreement measure obtained from the analysis was 0.754, ($p<0.001$), characterizing a very good agreement between observers. Conclusion: Single-pass total body CT split-bolus technique reached the highest overall image quality and an accurate TNM staging in pediatric patients with cancer.*

Correspondence to: Michele Scialpi MD, Associate Professor of Radiology, Radiology Division 2, Department of Surgical and Biomedical Sciences, Perugia University, S. Maria della Misericordia Hospital, S. Andrea delle Fratte, 06134, Perugia, Italy. Tel: +39 0755783507, Fax: +39 0755783488, e-mail: michelescialpi@libero.it; michelscialpi1@gmail.com

Key Words: Pediatric tumors, helical computed tomography (CT), multidetector-row CT (MDCT), radiation dose, split-bolus technique.

Development of advanced techniques, fast acquisition and radiation dose-modulation technologies has allowed an increased use of multi-detector computed tomography (MDCT) as diagnostic tool in infants and children (1), even though the information about examination protocols are scarce. Attention must be especially given to adapting protocols to suit children, taking into account that they are more sensitive to radiation than adults and that they have a longer life expectancy (2-4). International organizations and the U.S. Food and Drug Administration (FDA) have published a set of recommendations aimed at minimizing CT radiation doses to be as low as reasonably achievable, especially for children and small adults (5-8). Up to 31% of pediatric body computed tomography (CT) examinations are multi-phase, while others report portal-venous phase (1, 9, 10).

At our Institution, we replaced multiphasic and portal-venous phase (PVP) MDCT protocols at initial examination and follow-up of oncological pediatric patients by splitting the intravenous contrast material into two boli and combining phase images in a single scan ("split-bolus" MDCT protocol), with significant reduction of the required radiation dose (11).

The aim of the present study was to report an innovative protocol by split-bolus MDCT technique in children and small adults with cancer.

Patients and Methods

Patients. The study was retrospective and images were obtained for routine clinical examinations, therefore a formal approval of the Institutional Review Board of this study was not necessary. However, our Institutional Ethics Committee approved the use of this protocol of split-bolus MDCT in our oncologic patients (CEAS no. 1658/13/AV). Written informed consent for all included patients was given by the

Table I. *Split-bolus MDCT technique: total contrast medium volume related to patients weight, duration and flow rate for the first and second bolus of contrast material followed by saline solution.*

Patient weight (kg)	Contrast medium volume (ml)	1th Bolus (ml)/ flow rate (ml)	Saline (ml)/ flow rate (ml)	1th bolus duration (s)	2nd Bolus (ml)/ flow rate (ml)	Saline (ml)/ flow rate (ml)	2nd Bolus duration (s)	Total duration (s)
55	110	66/1.5	15/1.5	54	44/3.0	15/3.0	20	74
50	100	60/1.5	15/1.5	50	40/3.0	15/3.0	18	68
45	90	54/1.3	10/1.3	49	36/3.0	15/3.0	17	66
40	80	48/1.3	10/1.3	44.6	30/2.0	10/2.0	20	64.6
35	70	42/1.2	10/1.2	43.3	28/2.0	10/2.0	19	62.3
30	60	36/1.0	10/1.0	46	20/2.0	10/2.0	15	61
25	50	30/1.0	10/1.0	40	20/2.0	8/2.0	14	54
20	40	24/1.0	5/1.0	29	16/2.0	5/2.0	10.5	39.5
15	30	20/1.0	5/1.0	25	10/1.5	5/1.5	10	35
10	20	12/0.8	5/0.8	21	8/1.0	5/1.0	13	34
5	10	6/0.5	2/0.5	16	4/1.0	2/1.0	6	24

parents for the use for research purposes of their CT data. A total of 29 consecutive oncological patients (11 males and 18 females; age range=4 months to 16 years, mean age=9.3 years; weight between 5 and 55 kg, mean weight=36.2 kg), from June 2014 to September 2014, underwent split-bolus MDCT scanning of the chest, abdomen and pelvis as a part of initial MDCT (n=9) or follow-up (n=20).

All patients had histologically confirmed primary malignant cancer, typical of childhood: Hodgkin's (HL) and non-Hodgkin's lymphoma (NHL): n=14; neuroblastoma: n=5; Wilms' tumor: n=4; hepatoblastoma: n=1; osteosarcoma and Ewing's tumor: n=4; and rabdomiosarcoma (n=1). No patient had cardiovascular insufficiency.

Split-bolus MDCT protocol. All patients were scanned at two institutions by a Philips Brilliance 64-detector row scanner (Philips Healthcare, Best, the Netherlands). The scanning parameters were tube voltage, 80-100 kVp; a weight-based tube current adjustment from 30 to 140 mAs for each section; collimation, 64×0.625 mm; pitch, 0.935 without ECG gating; rotation time, 0.75 s; slice thickness, 2.0 mm; and reconstruction interval, 1.0 mm. The automatic online dose modulation (Z-DOM Brilliance 640; Philips Medical Systems Nederland) was then turned on. Another set of images was reconstructed for pulmonary parenchyma. MDCT examinations were completed with sagittal, coronal and curved multiplanar reconstructions (MPR).

Our protocol consisted of a single acquisition of the chest, abdomen and pelvis after intravenous (*i.v.*) injection of contrast material (350 mgI/ml Iomeron-Bracco Milano, Italy; 320 mg/ml Visipaque-GE Healthcare, Princeton, New Jersey, USA), split into two boli (Figure 1) by a power injector (Stelland CT; Medrad, Indianola, PA, USA) attached to two syringes, one containing contrast medium and one containing saline flush solution connected to a 20-24 G needle by a three-way stopcock.

The volume of contrast medium, duration of injection for the first and second bolus of contrast material and total injection time, related to patient weight and established on the basis of broad clinical experience and literature data (11-16), are reported in Table I.

The first bolus of contrast medium (1.2 ml/kg), at flow rate ranged from 0.5 to 1.5 ml/s allowed adequate parenchymal and venous enhancement (*e.g.* hepatic parenchymal during PVP). The injection duration of the first bolus of contrast medium including saline solution at the same flow rate and ranged from 5 to 15 ml. The second bolus of contrast medium (0.8 ml/kg) at a flow rate of 1-3 ml/s was used to obtain the hepatic arterial phase (HAP).

Using the scout film, a scan range from the pulmonary apex or diaphragm to the pubic symphysis was determined. Then the region of interest (ROI) of the bolus-tracking technique [raising the threshold value to 500 Hounsfield units (HU)] was placed on the descending aorta. After contrast injection of the first bolus of contrast material, bolus-tracking was initiated and when the ROI indicated the arrival of the contrast material in the aorta, the scan was started cranio-caudally after at least 6 s from the arrival of the contrast in the aorta. The inherent 6 s delay in the bolus-tracking technique is necessary to move the scan table to the start of the scan, give breath-hold instructions to the patient, and tune the gantry parameters. A single contrast-enhanced acquisition of the chest, abdomen and pelvis was obtained, resulting in a simultaneous contrast enhancement of the arterial and venous system.

Image analysis. All CT images were retrieved from the Institutional image archiving and communication system (PACS; Agfa Impax RIS Healthcare, Mortsel, Belgium, EU) and displayed and reviewed on a clinical workstation. Mean attenuations of the aorta at level of the celiac trunk, main portal vein and right lobe of the liver and renal cortex were measured using a circular ROI cursor by radiologists with experience in interpreting body CT images. CT attenuation values of hepatic parenchyma were measured in two areas (right posterior and left lateral segments) and averaged. Any focal parenchymal lesion, blood vessel, or artifact was carefully excluded from areas of hepatic attenuation measurement.

All CT images were reviewed in consensus by two radiologists (almost 25 and 5 years of experience in interpreting whole-body CT images). Assessments were based on the diagnostic quality of images of the entire mediastinum (analysis of both vascular and nonvascular structures), aorta, main portal vein, liver, renal cortex and pancreas. Qualitatively, the images were analyzed in relation to the TNM: detection and delineation of the primary tumor (assessment of the extent of the lesion to neighboring tissues), regional lymph nodes and distant metastasis.

Image quality was rated on the following 5-point scale: 1: excellent (excellent definition of tumor/metastases, excellent delineation of the

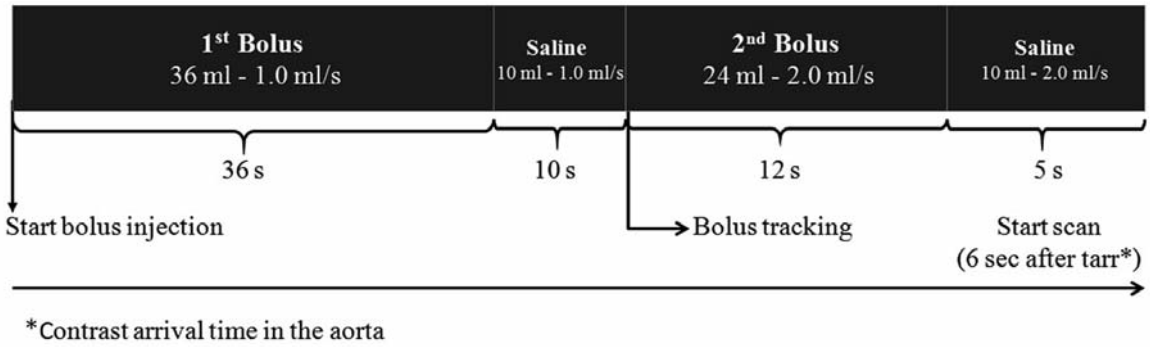

Figure 1. *Schematic view of split bolus 64-detector row computed tomographic scanning of the chest abdomen and pelvis in a 30 kg patient. First bolus [at the start of bolus injection (or time zero)]: 36 ml of contrast medium at 1.0 ml/s, followed by 10 ml of saline solution at the same flow rate, was injected to obtain adequate parenchymal and venous system enhancement. Second bolus: 24 ml of contrast medium at 2.0 ml/s followed by 10 ml of saline solution at the same flow rate to obtain hepatic arterial phase. We used bolus tracking (raising the threshold value at 500 HU) set with a circular region of interest placed on the descending aorta. Scan started cranio-caudally from the pulmonary apex to the pubic symphysis after a delay of at least 6 s from the arrival of the contrast medium in the aorta. A single acquisition was performed, resulting in simultaneous contrast enhancement of the arterial and venous system.*

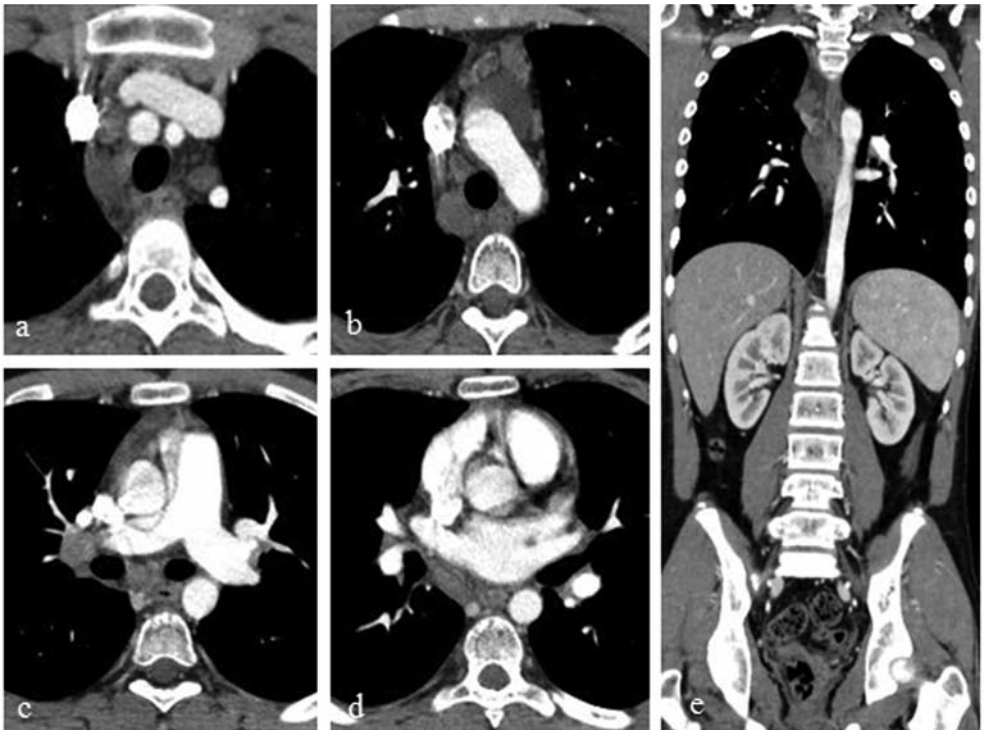

Figure 2. *Split-bolus of the chest abdomen and pelvis in a 14-year-old male (weight 50 kg) with non-Hodgkin lymphoma revealing lymph nodes in the mediastinum and in the right hilum (a-d). Note the optimal enhancement of the mediastinal arteries and veins. Coronal multiplanar reconstruction (e).*

structures); 2: good (good definition of tumor/metastases, minimal image noise); 3: adequate (adequate definition of tumor/metastases, slight impact of image noise, sufficient for diagnosis); 4: poor (poor definition of tumor/metastases, low attenuation and difficult delineation of the structures, increased image noise, diagnostic confidence reduced); 5: unacceptable/non-diagnostic.

Factors reducing image quality (obesity, motion, metallic artifacts, contrast medium flow-related, and contrast timing) were recorded by the radiologists.

As reported in the literature (17-20), the criterion used at our Institution to define optimal opacification were values of 149 HU or greater for the aorta at the level of celiac trunk, 141 HU for the

Figure 3. *Split-bolus of the chest abdomen and pelvis in a 4-year-old female (weight 15 kg) with neuroblastoma showing retroperitoneal periaortic solid tissue containing calcification with encasement of the renal arteries (arrows in a, b). Coronal multiplanar reconstruction (c) demonstrated the cranio-caudal extension of the lesions (arrows).*

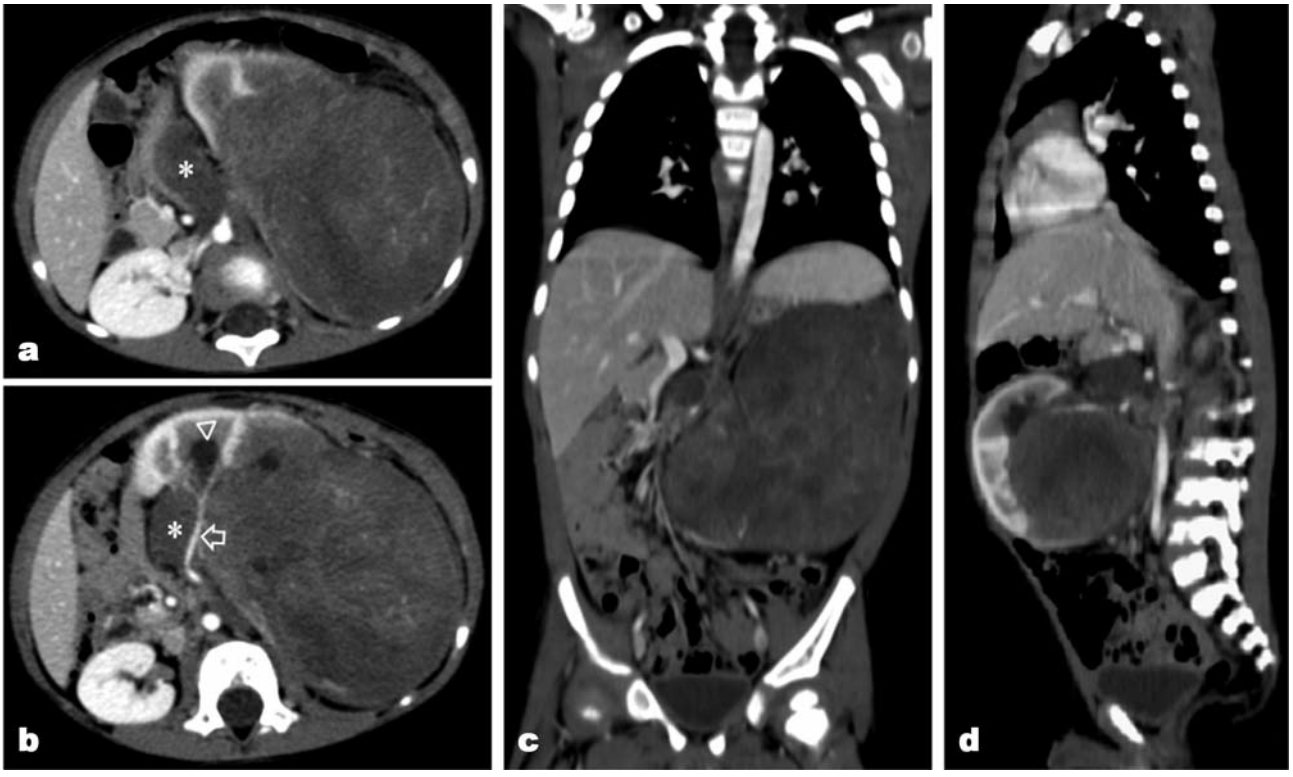

Figure 4. *Split-bolus of the chest abdomen and pelvis in a 2-year-old boy (weight 12 kg) with Wilms' tumor in the left kidney showing the voluminous mass of the left kidney with controlateral displacement beyond the midline. Note massive thrombosis of the right renal vein (*in a,b), calycectasia (head arrow in b), displacement of the left renal artery (arrow in b), and extension of the tumor in coronal (c), and sagittal (d) multiplanar renconstructions. No involvement of the lymph nodes was seen.*

main portal vein, 116 HU for the right lobe of the liver, 197 HU for the renal cortex and 121 HU for pancreatic parenchyma. In solid organs, the ROI was chosen in an area of parenchyma that had maximal density, and were free of injury, vessels, and artifacts. Mean and standard deviation (SD) enhancement values were calculated for combined HAP/PVP split-bolus protocol.

The appearance of parenchymal focal lesions at single-pass split-bolus MDCT was described on the basis of the attenuation and homogeneity of the lesion according to the typical features at multiphasic MDCT reported in the literature (11). The standard of reference for focal parenchymal lesions was given by biopsy results and clinical-imaging follow-up, of at least six months.

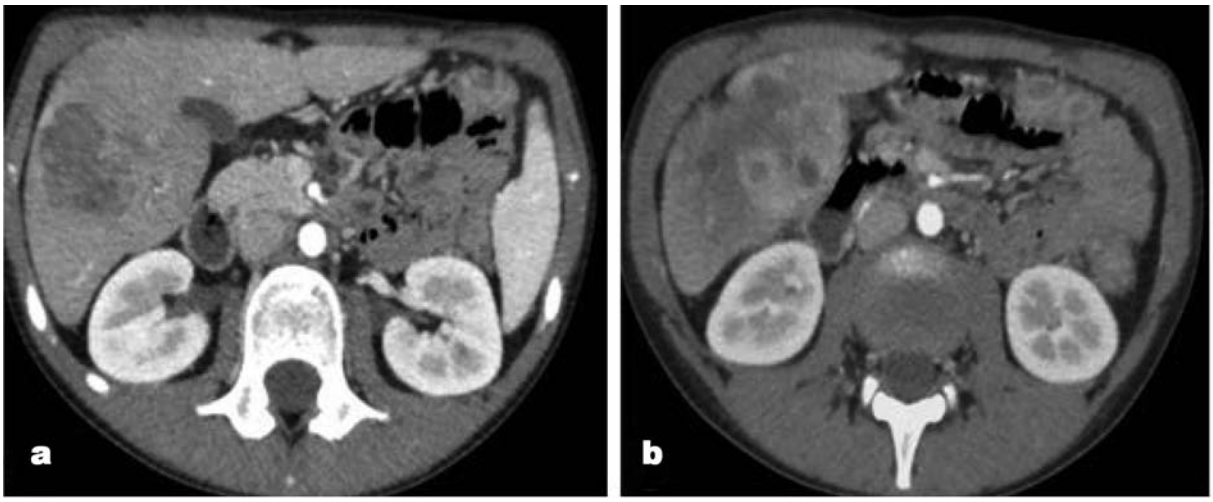

Figure 5. *Split-bolus of the chest abdomen and pelvis in a 14-year-old male (weight 51kg) with hepatoblastoma showing a voluminous inhomogenous mass in the right lobe of the liver (a, b).*

Statistical analysis. Statistical analysis was performed by using a commercially available software package (SPSS for Windows, version 15.0, Chicago, Illinois, USA). Agreement of both reviewers on image quality was assessed with linear weighted kappa statistics or using the Wilcoxon Mann-Whitney *U*-test as the data were nonparametric. The strength of agreement was categorized as non diagnostic or slight (κ= 0.00-0.20), poor or fair (κ=0.21-0.40), regular or moderate (κ=0.41-0.60), very good or substantial (κ=0.61-0.80), almost excellent/perfect to perfect (κ=0.81-1.00) according to Cohen and Fleiss kappa statistic method. A confidence interval (CI) of 95% was considered.

Radiation dose analysis. The dosimetric evaluation was carried out by analyzing the split-bolus MDCT examinations of all patients included in the study. Radiation dose was based on volume CT dose index (CTDIvol) and dose-length product (DLP) which were evaluated using the patient protocol saved in our PACS system after each examination. The effective dose (ED, in Sv) was calculated using the following equation: ED=k×DLP, where k=conversion coefficient. We used the conversion coefficient reported in literature (21-23). The calculated dose for the split-bolus was compared with that of the standard CT protocol previously used in the literature (24) for examination of pediatric patients.

Results

The MDCT split-bolus protocol allowed for images of high quality and accurate TNM staging in all cases (29/29).

In 14 patients with HL (n=5) and NHL (n=9) (Figure 2), staging was performed according to the Ann Arbor Staging classification and the St. Jude Children's Research Hospital Staging Classification, respectively (25-27). Mediastinal lymph nodes were revealed in HL (n=5) and NHL (n=6) and enlarged abdominal and pelvic nodes in NHL (n=3).

In the staging of patients with abdominal neuroblastoma (n=3) (Figure 3), according to the International Society of Pediatric Oncology Europe Neuroblastoma Group (SIOPEN) classifying locoregional tumors as resectable or unresectable on the basis of the presence of absence of a series of "imagine-defined risk factors" (IDRFs) detected with CT (28), independently of stage, tumor was unresectable in all cases. CT accurately defined tumor size and the relationship between the mass and adjacent structures in all cases. IDRFs (encasement or neighboring structure surrounded by the mass) of the aorta, celiac axis, mesenteric artery and vein, right renal pedicles were accurately assessed in all cases; compression of the inferior *vena cava* was observed in one case. No metastases of the bone, lymph nodes, liver, lung or pleura were revealed.

Wilm's tumor (n=4) (Figure 4) was revealed bilaterally in one case, in the left kidney in two cases, and in the right kidney in one. Tumor appeared as a heterogeneous density mass with well-defined margins. The tumor size ranged from 12 to 18 cm in maximum diameter. In the Wilm's tumor of the left kidney, the tumor penetrated and trespassed extended beyond the renal capsule, with displacement of the pancreas, psoas muscle, splenic hilum, and diaphragm. On the right side, it reached the porta hepatis and compressed the inferior *vena cava*. Enlarged lymph nodes of the kidney hilum and the periaortic lymph nodes were revealed in one case. Massive thrombus in the renal vein (n=1), and involvement of more than one third of the kidney and calycectasia (n=4) were also revealed. No liver metastases were observed.

Hepatoblastoma (n=1) (Figure 5) was staged according to Roebuck *et al*. (29). The voluminous tumor with polylobulated contours with syncronous lesions were revealed in the right lobe of the liver. Extrahepatic disease and distant metastases were not observed. Values of laboratory data for the liver function were elevated.

In the staging of bone tumors, rhabdomyosarcoma (n=1) and osteosarcoma and Ewing's tumor (n=4), non-thoracic or abdominal distant metastatic disease (lung, liver, bones, bone marrow, lymph nodes) were revealed.

On 2 out of 29 cases, the images were relatively limited by the presence of respiratory motion artifacts, which, however, did not compromise the correct diagnosis.

The mean attenuation in the aorta, main portal vein, liver, renal cortex and pancreas were 302±110 HU, 231±71 HU, 126.8±26.7 HU, 231±76.7 HU, and 146±33 HU, respectively. The mean attenuation in the aorta, main portal vein, liver were similar to those obtained in adult patients with split-bolus protocol as previously reported in literature (11). On the image quality, the Kappa value for the interobserver agreement measure obtained from the analysis was 0.754 ($p<0.001$, 95% CI), characterizing a very good agreement between observers.

The mean effective radiation dose was calculated to be 8.2±5.4 mSv for our MDCT split-bolus protocol.

Discussion

The optimal scanning protocol in the TNM staging of tumor in pediatric patients by MDCT is still a point of debate (30). A multitude of CT protocols for tumor staging in pediatric patients are described in the literature (8, 31-33). Few of these protocols entail scanning patients before contrast and at multiple phases after the administration of *i.v.* contrast material (34). Pediatric patients are more sensitive to radiation than adults that they have a longer life expectancy. Several international organizations and the U.S. FDA recommend minimizing the radiation dose in MDCT (5-8). Optimization of the CT protocols in any dose-reduction program by reduction of the multiple phases of contrast enhancement is essential.

The split-bolus protocol has been proposed in adult patients for CT urography, with a variety of techniques, for pancreatic cancer and characterization of liver lesions in oncological patients involving a reduction of radiation dose by scanning the chest and abdomen or abdomen (11, 22, 35-37). At our institutions, we implemented an innovative split-bolus protocol for the initial CT staging and follow-up by 64-detector row CT in oncological pediatric patients to ensure diagnostic efficacy and to obtain reduction of the radiation dose. In a single-pass, the split-bolus protocol achieves combined arterial and venous vessel enhancement by splitting the *i.v.* contrast material into two boli.

We correlated the mean attenuation value in the aorta, main portal vein, liver, renal cortex, and pancreas obtained by split-bolus in our study with the standard CT protocol reported in the literature (11, 17, 36, 38, 39). The MDCT split-bolus protocol demonstrated that the mean attenuation in the aorta, main portal vein, liver, renal cortex and pancreas were substantially similar to or higher with respect to the corresponding values reported in the literature (11, 17, 18, 36, 38, 40-42). Although the amount of contrast medium in the first bolus (1.0 mg/ml) is less than the amount used in conventional CT protocols (1.5-2 mg/ml), we obtained adequate enhancement of the liver parenchyma. This is explained by the effect of re-circulation. In addition, consistent enhancement in the portal vein, renal cortex and pancreatic parenchyma was obtained. The second bolus allowed optimal enhancement of the aorta.

The diagnostic efficacy and simultaneously adequate enhancement of the parenchyma, veins and arteries contributed to an accurate TNM: detection and delineation of the primary tumor (assessment of the extent of the lesion to neighboring tissues), regional lymph nodes and distant metastasis in all cases.

The split-bolus MDCT protocol by a single-pass procedure exposed the patient to approximatively 8 mSv. This is comparable to the lower values reported in the literature data (range=6.8-20.5 mSv for the chest and abdomen) (24), with the advantages of a simultaneous contrast enhancement of the arterial and venous system and of a reduction in the number of images needing electronic archiving.

Our study has certain limitations. This was a retrospective study with a small number of patients. Furthermore, different amounts and concentrations of the contrast material in the split-bolus study and standard protocol at our hospital and literature were used because of the pediatric age of the patients. In the split-bolus protocol, in order to obtain adequate vascular and parenchymal enhancement, we used a relatively increased amount of contrast material (maximum 110 ml for both boli); however, the total amount never exceeded 2 ml/kg.

In conclusion, the split-bolus MDCT is a novel emerging injection protocol. Considering simultaneous and adequate vascular and parenchymal enhancement in single-pass imaging, the split-bolus MDCT protocol can be used in the clinical setting to replace multiphasic or PVP processes in pediatric patients with cancer.

References

1 Mettler FA, Wiest PW, Locken JA and Kelsey CA: CT scanning: patterns of use and dose. J Radiol Prot 20(4): 353-359, 2000.

2 Hall EJ and Brenner DJ: Cancer risks from diagnostic radiology. Br J Radiol *81*: 362-378, 2008.

3 Donnelly LF, Emery KH, Brody AS, Laor T, Gylys-Morin VM, Anton CG, Thomas SR and Frush DP: Minimizing radiation dose for pediatric body applications of single-d etector helical CT: strategies at a large Children's Hospital. Am J Roentgenol *176*: 303-306, 2001.

4 Frush D.P.: Pediatric CT: practical approach to diminish the radiation dose. Pediatr Radiol *32*: 714-717, 2002.

5 International Atomic Energy Agency. International Action Plan for the Radiological Protection of Patients. In: ConferenceBoGG, ed editors. Vienna: IAEA, pp. 1-9, 2002.

6 European Communities. European Guidelines on Quality Criteria for Computed Tomography. Luxembourg: European Communities, 1999.

7 Menzel HG, Schibilla H and Teunen D: European Guidelines on Quality Criteria for Computed Tomography. Publication no. EUR 16262 EN. Luxembourg: European Commission, 2000.

8 Food and Drug Administration: FDA public health notification: reducing radiation risk from computed tomography for pediatric and small adult patients. Pediatr Radiol *32*: 314-316, 2002.

9 Roebuck DJ: Assessment of malignant liver tumors in children. Cancer imaging *9*(Special issue A): 98-103, 2009.

10 Nievelstein RA, van Dam IM and van der Molen AJ: Multidetector CT in children: current concepts and dose reduction strategies. Pediatr Radiol *40*: 1324-1344, 2010.

11 Scialpi M, Palumbo B, Pierotti L, Gravante S, Piunno A, Rebonato A, D'Andrea A, Reginelli A, Piscioli I, Brunese L and Rotondo A: Detection and characterization of focal liver lesions by split-bolus multidetector-row CT: diagnostic accuracy and radiation dose in oncologic patients. Anticancer Res *34(8)*: 4335-4344, 2014.

12 Ruess L, Bulas DI, Kushner DC, Silverman PM and Fearon TC: Peak enhancement of the liver in children using power injection and helical CT. AJR Am J Roentgenol *170*: 677-681, 1998.

13 Tsai IC, Lee T, Chen MC, Tsai WL, Lin PC and Liao WC: Homogeneous enhancement in pediatric thoracic CT aortography using a novel and reproducible method: contrast-covering time. Am J Roentgenol *188*: 1131-1137, 2007.

14 Frush DP, Spencer EB, Donnelly LF, Zheng Jy, DeLong DM and Bisset GS III: Optimizing contrast-enhanced abdominal CT in infants and children using bolus-tracking. Am J Roentgenol *172*: 1007-1013, 1999.

15 Frush DP: MDCT in children: scan techniques and contrast issues. In: Multidetector CT: From Protocols to Practice, First Edition. Kalra MK, Sanjay S and Rubin GD (eds.). Springer Verlag, Heidelberg, pp. 331-351, 2008.

16 Frush DP: Pediatric abdominal CT angiography. Pediatr Radiol *38*: 259-266, 2008.

17 Bae KT, Shah AJ, Shang SS *et al*. Aortic and hepatic contrast enhancement with abdominal 64-MDCT in pediatric patients: effect of body weight and iodine dose. Am J Roentgenol *191(5)*: 1589-1594, 2008.

18 Scialpi M, Cagini L, Pierotti L, De Santis F, Pusiol T, Piscioli I, Magli M, D'Andrea A, Brunese L and Rotondo A: Detection of small (≤2 cm) pancreatic adenocarcinoma and surrounding parenchyma: correlations between enhancement patterns at triphasic MDCT and histologic features. BMC Gastroenterol *21*: 14-16, 2014.

19 Rengo M, Caruso D, De Cecco CN, Lucchesi P, Bellini D, Maceroni MM, Ferrari R, Paolantonio P, Iafrate F, Carbone I, Vecchietti F and Laghi A: High concentration (400 mg/ml) versus low concentration (320 mg/ml) iodinated contrast media in multi detector computed tomography of the liver: a randomized, single centre, non-inferiority study. Eur J Radiol *81(11)*: 3096-101, 2012.

20 Tsuge Y, Kanematsu M, Goshima S, Kondo H, Hoshi H, Yokoyama R, Miyoshi T, Onozuka M, Moriyama N and Bae KT: Optimal scan delays for multiphasic renal multidetector row computed tomography performed with fixed injection duration of contrast medium. J Comp Assist Tomogr *33(1)*: 101-105, 2009.

21 Deak PD, Smal Y and Kalender WA: Multisection CT Protocols: Sex- and Age-specific Conversion Factors Used to Determine Effective Dose from Dose-Length Product; Radiology *257(1)*: 158-166, 2010.

22 The 2007 recommendations of the International Commission on Radiological Protection. ICRP publication 103. Ann ICRP *37(2-4)*: 1-332, 2007.

23 Thomas KE and Wang B: Age-specific effective doses for pediatric MSCT examinations at a large children's hospital using DLP conversion coefficients: a simple estimation method. Pediatr Radiol *38(6)*: 645-656, 2008.

24 Mahesh M: Advances in CT technology and application to pediatric imaging: Pediatr Radiol *41(2)*: 493-497, 2011.

25 Carbone PP, Kaplan HS, Musshoff K, Smithers DW and Tubiana M: Report of the Committee on Hodgkin's Disease Staging Classification. Cancer Res *31(11)*: 1860, 1971.

26 Lister TA, Crowther D, Sutcliffe SB, Glatstein E, Canellos GP, Young RC, Rosenberg SA, Coltman CA and Tubiana M: Report of a committee convened to discuss the evaluation and staging of patients with Hodgkin's disease: Cotswolds meeting. J Clin Oncol *7(11)*: 1630, 1989.

27 Murphy SB, Fairclough DL, Hutchison RE and Berard CW: Non-Hodgkin's lymphomas of childhood: an analysis of the histology, staging and response to treatment of 338 cases at a single institution. J Clin Oncol *7*: 186-193, 1989.

28 Monclair T, Brodeur GM, Ambros PF, Hervé JB, Cecchetto G, Holmes K, Kaneko M, London WB, Matthay KK, Nuchtern JG, von Schweinitz D, Simon T, Cohn SL and Pearson ADJ: The international neuroblastoma risk group (INRG) staging system: an INRG task force report. J Clin Oncol *27(2)*: 298-303, 2009.

29 Roebuck DJ, Aronson D, Clayput P, Czauderna P, de Ville de Goyet J, Gauthier F, MacKinlay G, Maibach R, McHugh K, Olsen ØE, Otte JB, Pariente D, Plaschkes J, Childs M and Perilongo G: 2005 PRETEXT: a revised staging system for primary malignant liver tumors of childhood developed by the SIOPEL group. Pediatr Radiol *37*: 123-32, 2007.

30 ACR-ASER-SCBT-MR-SPR practice parameter for the performance of pediatric computed tomography. 2014.

31 Siegel MJ: Practical CT techniques. In: Siegel MJ (ed) Pediatric body CT, 2nd Lippincott Williams & Wilkins, Philadelphia, pp. 1-32, 2008.

32 Frush DP and Donnelly LF: Helical CT in children: technical considerations and body applications. Radiology *209*: 37-48, 1998.

33 Frush DP, Donnelly LF and Rosen NS: Computed tomography and radiation risks: what pediatric health care providers should know. Pediatrics *112*: 951-957, 2003.

34 Dong Q and Chen J: CT Scan of Pediatric Liver Tumors, CT Scanning-Techniques and Apllications, Dr. Karupppasamy Subburaj (Ed.), ISBN: 978-953-307-943-1, InTech, Available from: http://www.intechopen.com/books/ct-scanning-techniques-and-applications/ct-scan-of-pediatric-liver-tumors, 2011.

35 Dillman JR, Caoli EM, Cohan RH, Ellis JH, Francis IR, Nan B and Zhang Y: Comparison of urinary tract distension and opacification using single-bolus 3-phase *vs*. split-bolus 2-phase multidetector row CT urography. J Comput Assist Tomogr *31(5)*: 750-757, 2007.

36 Brook OR, Gourtsoyianni S, Brook A, Siewert B, Kent T and Raptopoulos V: Spectral multidetector CT of the pancreas: assessment of radiation dose and tumor conspicuity. Radiology *269(1)*: 139-148, 2013.

37 Scialpi M, Piscioli I, Magli M and D'Andrea A: Split-bolus spectral multidetector CT of the pancreas: problem solving in the detection of "isoattenuating" pancreatic cancer? Radiology *270(3)*: 936-937, 2014.

38 Bae KT: Intravenous contrast medium administration and scan timing in CT: considerations and approaches. State of the art. Radiology *256*: 32-61, 2010.

39 Goshima S, Kanematsu M, Nishibori H, Kondo H, Tsuge Y, Yokoyama R, Miyoshi T, Onozuka M, Shiratori Y, Moriyama N and Bae KT: Multi-detector row CT of the kidney: Optimizing scan delays for bolus tracking techniques of arterial, corticomedullary, and nephrographic phases. Eur J Radiol *63*: 420-426, 2007.

40 Kekelidze M, Dwarkasing RS, Dijkshoorn ML, Sikorska K, Verhagen PC and Krestin GP: Kidney and urinary tract imaging: triple-bolus multidetector CT urography as a one-stop shop page 24 of 24 protocol design, opacification, and image quality analysis. Radiology *255*: 508-516, 2010.

41 Chow LC, Kwan SW, Olcott EW and Sommer G: Split-bolus MDCT urography with synchronous nephrographic and excretory phase enhancement. Am J Roentgenol *189*: 314-322, 2007.

42 Maheshwari E, O'Malley ME, Ghai S, Staunton M and Massey C: Split-bolus MDCT urography: upper tract opacification and performance for upper tract tumors in patients with hematuria. Am J Roentgenol *194*: 453-458, 2010.

Received January 4, 2015
Revised February 5, 2015
Accepted February 9, 2015